another FLT3/ITD-positive AML cell line (top panel of Figure 5a lane 4 and 6 vs lane 1 and 3), although STAT5 phosphorylation was inhibited similarly to the condition without FLT3 ligand (third panel of Figure 5a lane 4 and 6 vs lane 1 and 3). Consistently, the sensitivity of MOLM13 cells to sunitinib fell with FLT3 ligand (Figure 5b). On the other hand, OPB-31121 induced strong inhibition of both STAT3 and STAT5 phosphorylation independently of FLT3 ligand presence (Figure 5a lane 1 and 2 vs lane 4 and 5), and the growth inhibitory effect of this compound on MOLM13 was hardly affected by the addition of FLT3 ligand (Figure 5c). These results indicated that this compound overcame FLT3 ligand-induced FLT3 inhibitor resistance.

DISCUSSION

Constitutive activation of STAT3 and STAT5 has been reported in various cancers and the inhibition of STAT signaling has been thought to be a promising strategy for cancer therapy.[33–35] Many trials using several approaches, such as small molecules including upstream kinase inhibitors, STAT dimerization inhibitors, and STAT phosphorylation inhibitors, neutralizing antibody against upstream receptors and ligands, and decoy oligonucleotides, have been performed; however, very few of them demonstrated an *in vivo* effect in mouse models and none has undergone clinical trials, except upstream kinase inhibitors such as JAK inhibitors.[22] To the best of our knowledge, OPB-31121 is the first STAT inhibitor to undergo phase I trials.

The mechanism of action of OPB-31121 has not been fully revealed. This compound did not have kinase inhibitory activity against any kinase (Supplementary Table S1) and inhibited STAT3 and STAT5 phosphorylation without inhibition of JAK2 and SFKs (Figures 2a–c). This compound did not inhibit nuclear translocation of STAT3 after it was phosphorylated (Figure 1c) and did not disrupt the dimerization of STAT3 (data not shown). In addition, this compound did not induced the protein expression of JAK-STAT pathway negative regulators such as suppressor or cytokine signaling (SOCS)3, protein inhibitor of activated Stats (PIAS)4 and LNK (data not shown). These data indicated that this compound did not inhibit the phosphorylation of upstream kinases but inhibited STAT phosphorylation, most likely by inhibiting the association of STAT with JAK or cytokine receptors; however, this

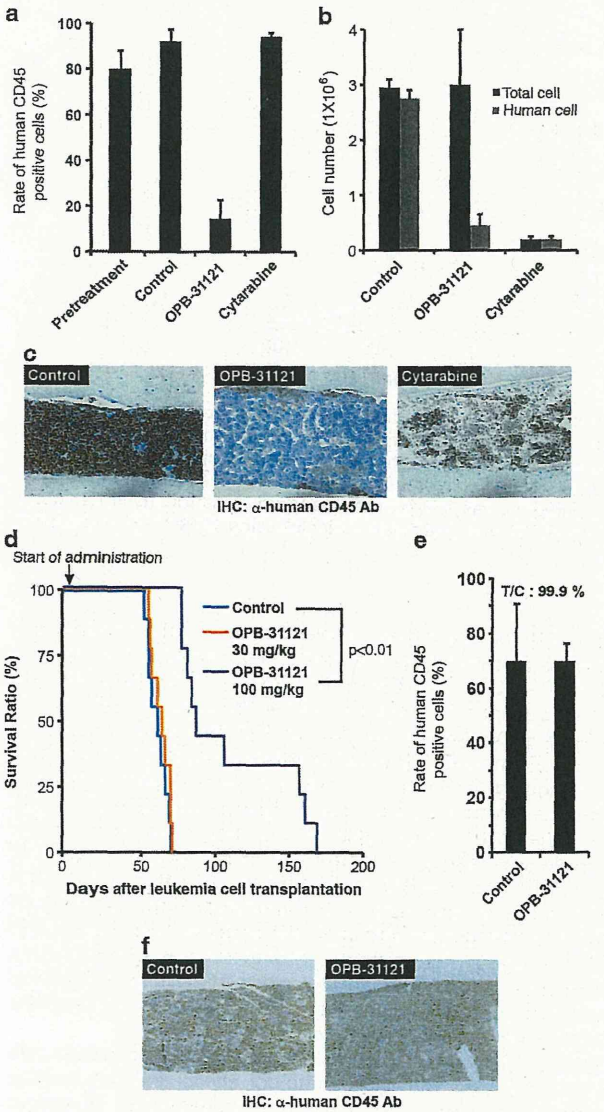

g

Summary of OPB-31121 effect on primary leukemia and normal hematopoietic cells

Sample	Disease	SAO	Duration	Dose (mg/kg)	T/C (%)
OMR	ALL	BCR-ABL	Day 23-32	200	4
ARK	ALL	BCR-ABL	Day 18-31	300	58
KWI	ALL	BCR-ABL Y253H	Day 45-54	200	57
INH	CML BC	BCR-ABL T315I	Day 21-30	200	87
			Day 1-29	200	15.3
MAE	AML	FLT3/ITD	Day 29-38	200	15.9
MIZ	AML	FLT3/ITD	Day 40-49	200	26.3
CB	Normal	(-)	Day 50-59	200	99.9

Figure 4. OPB-31121 selectively reduced human primary leukemia cells in mice. MAE cells (1×10^6), primary FLT3/ITD-positive human AML cells, were intravenously transplanted into NOG mice. On day 29, the rate of human leukemia cells in femoral bone marrow of the pretreatment mice was measured by flow cytometry using anti-human CD45 antibody, and daily oral administration of 5% gum arabic or OPB-31121 (200 mg/kg) for 10 days was started. On day 32, daily intraperitoneal injection of cytarabine (400 mg/kg) for 7 days was started. On day 38, bone marrow cells were collected from one femur and the other femur was fixed and subjected to immunohistochemistry with anti-human CD45 antibody. The rate of human leukemia cells in bone marrow was analyzed as above. (**a**) The average human leukemia cell rate of three mice was plotted on the bar chart with standard deviation. (**b**) Bone marrow cells collected from a femur were counted. The leukemia cell number was calculated by multiplying the total cell number by the human CD45-positive cell rate. The average value of three mice was plotted on the bar chart with standard deviation. OPB-31121 did not reduce the total cell number. (**c**) Immunohistochemistry of bone marrow with anti-human CD45 antibody. Cells stained in brown and blue were human CD45-positive cells (leukemia cells) and negative cells (mouse normal hematopoietic cells), respectively. Normal hematopoietic cells recovered by OPB-31121 treatment. (**d**) Survival benefit of OPB-31121 treatment in mice transplanted with primary CML BC cells harboring BCR–ABL T315I. INH cells (5×10^6), primary BCR–ABL T315I-positive CML BC cells, were intravenously transplanted into NOG mice. Daily oral administration of 5% gum arabic or the indicated dose of OPB-31121 was started on day 2 and continued until mice died. Each group consisted of nine mice. Survival curve were plotted according to the Kaplan–Meier method. Statistical difference of survival was analyzed by the log-rank test. (**e**) OPB-31121 did not affect the growth of normal hematopoietic cells. CD34-positive human cord blood cells (1×10^5) were transplanted, treated and analyzed as described above except that mice were irradiated (2.5 Gy) the day before transplantation and that OPB-31121 and gum arabic were administered daily from days 50–59. The average human cell rate of two mice was plotted on the bar chart with standard deviation. (**f**) Immunohistochemistry of bone marrow of mice transplanted with cord blood cells were performed as in (**c**). (**g**) Summary of OPB-31121 effect on primary leukemia and normal hematopoietic cells.

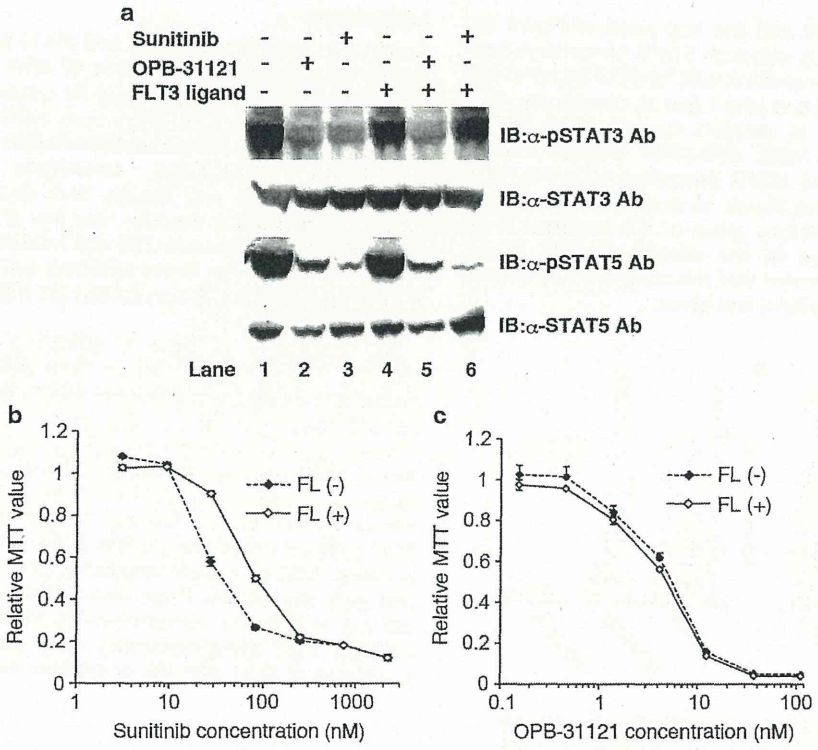

Figure 5. OPB-31121 overcame autocrine-induced FLT3 inhibitor resistance. (**a**) MOLM13 cells were treated with 100 nM sunitinib, 100 nM OPB-31121 and 100 ng/ml FLT3 ligand as indicated for 4 h. Then, cells were lysed and subjected to IB with the indicated antibodies. (**b**) FLT3 ligand reduced sunitinib sensitivity in MOLM13 cells. MOLM13 cells were cultured with the indicated dose of sunitinib with or without 100 ng/ml FLT3 ligand. Cell proliferation was analyzed by MTT assay after 48 h culture. MTT values were plotted as relative values to the value of the cells without FLT3 ligand and sunitinib. The average value of three experiments was plotted with standard deviation. (**c**) FLT3 ligand did not affect the sensitivity to OPB-31121 in MOLM13 cells. Sensitivity of OPB-31121 was measured as in (**b**) using OPB-31121 instead of sunitinib.

compound could not inhibit STAT3 phosphorylation by JAK2 and Lyn *in vitro*, suggesting that another cellular protein was required for this compound to inhibit STAT phosphorylation. This compound may indirectly bind to STAT through an unknown protein that interacts with STAT and disrupts the association of STAT with upstream kinases or receptors. We are now searching for the components of STAT complex that interact with this compound. Very recently, another group reported a decrease in the phosphorylation of STAT3 and JAK2 24 or 48 h after treatment with this compound in gastric cancer cell lines, and claimed that this compound was a JAK2 inhibitor;[25] however, we clearly demonstrated that the decrease in STAT3 phosphorylation occurred much earlier, within 2 h after treatment with this compound, and before the decrease in JAK2 and c-Src phosphorylation (Figures 2b and c). At 24 h after treatment, we also observed a decrease in JAK2 phosphorylation, probably due to the cell death response (Figure 2b). A similar phenomenon might have been observed in gastric cancer cell lines.

The sensitivity of cell lines to OPB-31121 varied markedly and was independent of the phosphorylation level of STAT (Table 1 and data not shown). This was probably because the survival dependency on STAT signaling varied among cell lines and was independent of the STAT phosphorylation level; therefore, it was difficult to predict OPB-31121-sensitive cells from the phosphorylation level of STAT. On the other hand, it is reasonable to predict a cancer to be addictive to STAT signaling, when the cancer gets addicted to an oncokinase, and the survival supporting activity of the oncokinase depend on STAT signaling. It is also difficult to clarify whether a mutated kinase observed in a cancer is really responsible for cancer cell survival through STAT signaling, but numerous past studies have proved it in some oncokinaes such as SAO (BCR–ABL, FLT3/ITD and JAK2 V617F).[17,30,31] Therefore, we selected SAO-positive leukemia cells as the target of OPB-31121. Strikingly, SAO-positive leukemia cells, including primary leukemia cells, were generally OPB-31121 sensitive both *ex vivo* and *in vivo*. It is intriguing that OPB-31121 did not cause growth inhibition of normal hematopoietic cells (Figures 5b, c, e and f). In fact, the dose-limiting toxicity of this compound did not show hematological toxicity in phase I trial with a maximum dose of 800 mg/kg.[29] No hematological toxicity was observed in the toxicity study of this compound in monkeys (1000 mg/kg for 14 days, data not shown). Although the importance of STAT3 and STAT5 in various signals from cytokines such as erythropoietin, thrombopoietin and granulocyte-colony stimulating factor has been established, the dependence on STAT signaling will be lower in normal hematopoietic cells than in malignant cells.

Specific inhibitors of kinases aberrantly activated in tumor cells are powerful tools with high antitumor effects and less toxicity; however, cancer cells sometimes develop resistance in various ways. CML cells are reported to develop the resistance to ABL kinase inhibitor by a drug-resistant mutation in BCR–ABL, overexpression of BCR–ABL,[36] overexpression of Lyn as an alternative activator of STAT5[37] and STAT3 activation through an alternative signal from bone marrow stroma cells.[38] In FLT3/ITD-positive AML cells, resistance to FLT3 inhibitor was achieved by a drug-resistant mutation in FLT3, overexpression of FLT3 and autocrine Flt3 ligand stimulation.[32,39] In JAK2 V617F-positive AML or polycythemia vera, specific JAK2 inhibition was overcome by

alternative activation of other JFKs.[23] The mechanisms of drug resistance are various but many of them finally lead to the maintenance of STAT3/5 activation. This is probably because SAO-positive leukemia cells require the maintenance of STAT3/5 activation for drug-resistant survival; therefore, it is a reasonable strategy to overcome SAO inhibitor resistance by a STAT inhibitor. We showed examples of this strategy in the case of a drug-resistant mutation in BCR–ABL and autocrine-induced FLT3 inhibitor resistance (Figures 4d and 5a–c).

Taken together, we conclude that OPB-31121 holds promise as a non-myelosuppressive therapeutic agent against a wide range of hematopoietic malignancies, especially SAO-positive leukemia. As OPB-31121 showed strong antitumor effects also in a wide range of solid tumors (data not shown), two phase I studies have been performed on advanced solid tumors in Korea (NCT00955812) and for non-Hodgkin's lymphoma and multiple myeloma in Hong Kong (NCT00511082), and the results are awaited. A phase I/II study of hepatocellular carcinoma in Japan (NCT1406574) is ongoing.

CONFLICT OF INTEREST

TN received research funding from Otsuka Pharmaceutical Co., Ltd, Kyowa Hakko Kirin Co., Ltd., Wyeth and Chugai Pharmaceutical Co., Ltd. KS, YH, NH and NO are employees of Otsuka Pharmaceutical Co., Ltd., whose product was studied in this work. The other authors declare no conflict of interest.

ACKNOWLEDGEMENTS

We thank Dr Takeyama for generously providing the cell lines. We are very grateful to Yoko Matsuyama, Asako Watanabe and Chika Wakamatsu for their technical assistance. This work was supported by MHLW KAKENHI Grant Number H22-3jigan-Ippan-010 and JSPS KAKENHI Grant Numbers 23591381, 25293218, and 23659487.

AUTHOR CONTRIBUTIONS

FH designed the research, performed experiments and wrote the paper. KS designed the research and performed experiments. YH, NH, NO and SK performed experiments. TN designed the research.

REFERENCES

1 Ihle JN. STATs: signal transducers and activators of transcription. *Cell* 1996; **84**: 331–334.
2 Leonard WJ, O'Shea JJ. Jaks and STATs: biological implications. *Annu Rev Immunol* 1998; **16**: 293–322.
3 Hayakawa F, Naoe T. SFK-STAT pathway: an alternative and important way to malignancies. *Ann NY Acad Sci* 2006; **1086**: 213–222.
4 Chen X, Vinkemeier U, Zhao Y, Jeruzalmi D, Darnell JE, Kuriyan Jr J. Crystal structure of a tyrosine phosphorylated STAT-1 dimer bound to DNA. *Cell* 1998; **93**: 827–839.
5 Shuai K, Horvath CM, Huang LH, Qureshi SA, Cowburn D, Darnell Jr JE. Interferon activation of the transcription factor Stat91 involves dimerization through SH2-phosphotyrosyl peptide interactions. *Cell* 1994; **76**: 821–828.
6 Bromberg JF, Horvath CM, Besser D, Lathem WW, Darnell Jr JE. Stat3 activation is required for cellular transformation by v-src. *Mol Cell Biol* 1998; **18**: 2553–2558.
7 Turkson J, Bowman T, Garcia R, Caldenhoven E, De Groot RP, Jove R. Stat3 activation by Src induces specific gene regulation and is required for cell transformation. *Mol Cell Biol* 1998; **18**: 2545–2552.
8 Besser D, Bromberg JF, Darnell Jr JE, Hanafusa H. A single amino acid substitution in the v-Eyk intracellular domain results in activation of Stat3 and enhances cellular transformation. *Mol Cell Biol* 1999; **19**: 1401–1409.
9 Zong CS, Zeng L, Jiang Y, Sadowski HB, Wang LH. Stat3 plays an important role in oncogenic Ros- and insulin-like growth factor I receptor-induced anchorage-independent growth. *J Biol Chem* 1998; **273**: 28065–28072.
10 Migone TS, Lin JX, Cereseto A, Mulloy JC, O'Shea JJ, Franchini G *et al.* Constitutively activated Jak-STAT pathway in T cells transformed with HTLV-I. *Science* 1995; **269**: 79–81.
11 Weber-Nordt RM, Egen C, Wehinger J, Ludwig W, Gouilleux-Gruart V, Mertelsmann R *et al.* Constitutive activation of STAT proteins in primary lymphoid and myeloid leukemia cells and in Epstein-Barr virus (EBV)-related lymphoma cell lines. *Blood* 1996; **88**: 809–816.
12 Danial NN, Pernis A, Rothman PB. Jak-STAT signaling induced by the v-abl oncogene. *Science* 1995; **269**: 1875–1877.
13 Danial NN, Rothman P. JAK-STAT signaling activated by Abl oncogenes. *Oncogene* 2000; **19**: 2523–2531.
14 de Groot RP, Raaijmakers JA, Lammers JW, Jove R, Koenderman L. STAT5 activation by BCR-Abl contributes to transformation of K562 leukemia cells. *Blood* 1999; **94**: 1108–1112.
15 Nieborowska-Skorska M, Wasik MA, Slupianek A, Salomoni P, Kitamura T, Calabretta B *et al.* Signal transducer and activator of transcription (STAT)5 activation by BCR/ABL is dependent on intact Src homology (SH)3 and SH2 domains of BCR/ABL and is required for leukemogenesis. *J Exp Med* 1999; **189**: 1229–1242.
16 Sillaber C, Gesbert F, Frank DA, Sattler M, Griffin JD. STAT5 activation contributes to growth and viability in Bcr/Abl-transformed cells. *Blood* 2000; **95**: 2118–2125.
17 Hayakawa F, Towatari M, Kiyoi H, Tanimoto M, Kitamura T, Saito H *et al.* Tandem-duplicated Flt3 constitutively activates STAT5 and MAP kinase and introduces autonomous cell growth in IL-3-dependent cell lines. *Oncogene* 2000; **19**: 624–631.
18 Mizuki M, Fenski R, Halfter H, Matsumura I, Schmidt R, Muller C *et al.* Flt3 mutations from patients with acute myeloid leukemia induce transformation of 32D cells mediated by the Ras and STAT5 pathways. *Blood* 2000; **96**: 3907–3914.
19 Lu X, Levine R, Tong W, Wernig G, Pikman Y, Zarnegar S *et al.* Expression of a homodimeric type I cytokine receptor is required for JAK2V617F-mediated transformation. *Proc Natl Acad Sci USA* 2005; **102**: 18962–18967.
20 Bromberg JF, Wrzeszczynska MH, Devgan G, Zhao Y, Pestell RG, Albanese C *et al.* Stat3 as an oncogene. *Cell* 1999; **98**: 295–303.
21 Onishi M, Nosaka T, Misawa K, Mui AL, Gorman D, McMahon M *et al.* Identification and characterization of a constitutively active STAT5 mutant that promotes cell proliferation. *Mol Cell Biol* 1998; **18**: 3871–3879.
22 Yue P, Turkson J. Targeting STAT3 in cancer: how successful are we? *Exp Opin Invest Drug* 2009; **18**: 45–56.
23 Koppikar P, Bhagwat N, Kilpivaara O, Manshouri T, Adli M, Hricik T *et al.* Heterodimeric JAK-STAT activation as a mechanism of persistence to JAK2 inhibitor therapy. *Nature* 2012; **489**: 155–159.
24 Shiotsu Y, Kiyoi H, Ishikawa Y, Tanizaki R, Shimizu M, Umehara H *et al.* KW-2449, a novel multikinase inhibitor, suppresses the growth of leukemia cells with FLT3 mutations or T315I-mutated BCR/ABL translocation. *Blood* 2009; **114**: 1607–1617.
25 Kim MJ, Nam HJ, Kim HP, Han SW, Im SA, Kim TY *et al.* OPB-31121, a novel small molecular inhibitor, disrupts the JAK2/STAT3 pathway and exhibits an antitumor activity in gastric cancer cells. *Cancer Lett* 2013; **335**: 145–152.
26 Kurahashi S, Hayakawa F, Miyata Y, Yasuda T, Minami Y, Tsuzuki S *et al.* PAX5-PML acts as a dual dominant-negative form of both PAX5 and PML. *Oncogene* 2011; **30**: 1822–1830.
27 Tanizaki R, Nomura Y, Miyata Y, Minami Y, Abe A, Hanamura A *et al.* Irrespective of CD34 expression, lineage-committed cell fraction reconstitutes and re-establishes transformed Philadelphia chromosome-positive leukemia in NOD/SCID/IL-2Rgammac $-/-$ mice. *Cancer Sci* 2010; **101**: 631–638.
28 Okamoto M, Hayakawa F, Miyata Y, Watamoto K, Emi N, Abe A *et al.* Lyn is an important component of the signal transduction pathway specific to FLT3/ITD and can be a therapeutic target in the treatment of AML with FLT3/ITD. *Leukemia* 2007; **21**: 403–410.
29 Oh D, Han S, Kim TM, Lee S, Kim T, Heo DS *et al.* A phase I, open-label, non-randomized trial of OPB-31121, a STAT3 inhibitor, in patients with advanced solid tumors. *J Clin Oncol* 2010; **28**: e13056.
30 Levine RL, Wadleigh M, Cools J, Ebert BL, Wernig G, Huntly BJ *et al.* Activating mutation in the tyrosine kinase JAK2 in polycythemia vera, essential thrombocythemia, and myeloid metaplasia with myelofibrosis. *Cancer Cell* 2005; **7**: 387–397.
31 Carlesso N, Frank DA, Griffin JD. Tyrosyl phosphorylation and DNA binding activity of signal transducers and activators of transcription (STAT) proteins in hematopoietic cell lines transformed by Bcr/Abl. *J Exp Med* 1996; **183**: 811–820.
32 Zhou J, Bi C, Janakakumara JV, Liu SC, Chng WJ, Tay KG *et al.* Enhanced activation of STAT pathways and overexpression of survivin confer resistance to FLT3 inhibitors and could be therapeutic targets in AML. *Blood* 2009; **113**: 4052–4062.
33 Page BD, Ball DP, Gunning PT. Signal transducer and activator of transcription 3 inhibitors: a patent review. *Exp Opin Ther Patent* 2011; **21**: 65–83.
34 Lai SY, Johnson FM. Defining the role of the JAK-STAT pathway in head and neck and thoracic malignancies: implications for future therapeutic approaches. *Drug Resist Update Rev Comment Antimicrob Anticancer Chemother* 2010; **13**: 67–78.
35 Scuto A, Kujawski M, Kowolik C, Krymskaya L, Wang L, Weiss LM *et al.* STAT3 inhibition is a therapeutic strategy for ABC-like diffuse large B-cell lymphoma. *Cancer Res* 2011; **71**: 3182–3188.

36 Mahon FX, Deininger MW, Schultheis B, Chabrol J, Reiffers J, Goldman JM *et al.* Selection and characterization of BCR-ABL positive cell lines with differential sensitivity to the tyrosine kinase inhibitor STI571: diverse mechanisms of resistance. *Blood* 2000; **96**: 1070–1079.
37 Donato NJ, Wu JY, Stapley J, Gallick G, Lin H, Arlinghaus R *et al.* BCR-ABL independence and LYN kinase overexpression in chronic myelogenous leukemia cells selected for resistance to STI571. *Blood* 2003; **101**: 690–698.
38 Bewry NN, Nair RR, Emmons MF, Boulware D, Pinilla-Ibarz J, Hazlehurst LA. Stat3 contributes to resistance toward BCR-ABL inhibitors in a bone marrow microenvironment model of drug resistance. *Mol Cancer Ther* 2008; **7**: 3169–3175.
39 Kindler T, Lipka DB, Fischer T. FLT3 as a therapeutic target in AML: still challenging after all these years. *Blood* 2010; **116**: 5089–5102.

Supplementary Information accompanies this paper on Blood Cancer Journal website (http://www.nature.com/bcj)

Published OnlineFirst February 25, 2013; DOI: 10.1158/1541-7786.MCR-12-0544

Molecular Cancer Research

Oncogenes and Tumor Suppressors

CDCP1 Regulates the Function of MT1-MMP and Invadopodia-Mediated Invasion of Cancer Cells

Yuri Miyazawa[1], Takamasa Uekita[1], Yuumi Ito[1,2], Motoharu Seiki[3], Hideki Yamaguchi[1], and Ryuichi Sakai[1]

Abstract

Complement C1r/C1s, Uegf, Bmp1 (CUB) domain-containing protein 1 (CDCP1) is a transmembrane protein that regulates anchorage-independent growth and cancer cell migration and invasion. Expression of CDCP1 is detected in a number of cancer cell lines and tissues and is closely correlated with poor prognosis. Invadopodia are actin-based protrusions on the surface of invasive cancer cells that promote the degradation of the extracellular matrix (ECM) via localized proteolysis, which is mainly mediated by membrane type 1 matrix metalloproteinase (MT1-MMP). MT1-MMP is accumulated at invadopodia by targeted delivery via membrane trafficking. The present study shows that CDCP1 is required for ECM degradation by invadopodia in human breast cancer and melanoma cells. CDCP1 localized to caveolin-1–containing vesicular structures and lipid rafts and was detected in close proximity to invadopodia. Further biochemical analysis revealed that substantial amounts of CDCP1 existed in the Triton X-100 insoluble lipid raft fraction. CDCP1 was coimmunoprecipitated with MT1-MMP and colocalized with MT1-MMP at the vesicular structures. The siRNA-mediated knockdown of the CDCP1 expression markedly inhibited MT1-MMP–dependent ECM degradation and Matrigel invasion and reduced the accumulation of MT1-MMP at invadopodia, as shown by immunofluorescence analysis. These results indicate that CDCP1 is an essential regulator of the trafficking and function of MT1-MMP- and invadopodia-mediated invasion of cancer cells. *Mol Cancer Res; 11(6); 628–37.* ©*2013 AACR.*

Introduction

Complement C1r/C1s, Uegf, Bmp1 (CUB) domain-containing protein 1 (CDCP1), also described as SIMA135 and TRASK (1, 2), is a type 1 transmembrane protein with 3 CUB domains as the extracellular domains and several tyrosine residues that can be phosphorylated by Src family kinases (SFK) in the intracellular domain (1–6). The expression of CDCP1 was reported in several human malignancies, such as colon and breast cancers (3, 7). CDCP1 expression is strongly associated with cancer progression and poor prognosis in renal cell carcinoma, lung adenocarcinoma, and pancreatic cancer (8–10). We previously reported that CDCP1 is a critical regulator of anoikis resistance in lung cancer cells (11), peritoneal dissemination of gastric scirrhous carcinoma (12), and invasion of pancreatic cancer cells (8). We showed that knockdown of CDCP1 resulted in the inhibition of extracellular matrix (ECM) degradation by pancreatic cancer cells (8). Tyrosine phosphorylation of CDCP1, especially at tyrosine 734 residue, plays an essential role in these oncogenic processes (8, 11, 12). However, the exact molecular mechanisms by which CDCP1 regulates cancer cell invasion remain to be determined.

Matrix metalloproteinases (MMP) have been implicated in many aspects of cancer progression, such as tumor growth, angiogenesis, invasion, and metastasis (13). Among MMPs, membrane type 1 (MT1)-MMP, the first discovered membrane-type MMP (14), plays a pivotal role in ECM degradation at the leading edge of invasive cancer cells (15). Clinically, MT1-MMP expression is strongly associated with cancer progression and metastasis (16) and poor prognosis of patients (17, 18). A cell–surface complex consisting of MT1-MMP oligomers binds to inactive proMMP-2 and mediates its cleavage and activation (19). In addition to activating secreted MMPs, MT1-MMP plays a key role in cancer invasion through its interaction and processing of cell surface proteins including CD44 (20). MT1-MMP function can be regulated by clathrin-mediated or caveolar endocytosis followed by degradation in the lysosomal compartment (21).

Invadopodia are unique protrusions observed at the cell adhesion sites of invasive cancer cells that are rich in cell-ECM adhesion molecules, actin assembly regulators, membrane-remodeling proteins, tyrosine kinases, tyrosine-phosphorylated proteins, and MMPs (22, 23). Because they offer an environment that supports ECM

Authors' Affiliations: [1]Division of Metastasis and Invasion Signaling, National Cancer Center Research Institute; [2]Laboratry of Genome and Biosignal, Tokyo University of Pharmacy and Life Sciences; and [3]Division of Cancer Cell Research, Institute of Medical Science, The University of Tokyo, Tokyo, Japan

Corresponding Author: Ryuichi Sakai, National Cancer Center Research Institute, 5-1-1 Tsukiji, Chuo-ku, Tokyo 104-0045, Japan. Phone: 81-3-3547-5247; Fax: 81-3-3542-8170; E-mail: rsakai@ncc.go.jp

doi: 10.1158/1541-7786.MCR-12-0544

Published OnlineFirst February 25, 2013; DOI: 10.1158/1541-7786.MCR-12-0544

degradation and thus cancer invasion and metastasis, the ability to form invadopodia is closely associated with the invasive and metastatic potentials of cancer cells (24, 25). The matrix degradation activity at invadopodia is dependent on the accumulation and activation of MT1-MMP at the cell surface of invadopodia (26–28). Recent studies have revealed that endocytic and exocytic trafficking are critical for the targeted delivery of MT1-MMP to invadopodia (21, 29–31). However, the molecular mechanisms that control the delivery and function of MT1-MMP at invadopodia are not fully understood. In this study, we show that CDCP1 regulates the function of MT1-MMP and plays an essential role in ECM degradation at invadopodia in human cancer cells.

Materials and Methods

Cell culture and transfection

The human breast cancer cell line MDA-MB-231 and the human melanoma cell line RPMI 7951 were obtained from the American Type Culture Collection. MDA-MB-231 and RPMI 7951 cells were maintained in a 1:1 mixture of high-glucose Dulbecco's modified Eagle's medium and RPMI-1640 supplemented with 10% FBS, 10 U/mL penicillin, and 10 μg/mL streptomycin. The cells were transfected with the indicated plasmids, using Lipofectamine 2000 or Lipofectamine LTX (Life Technologies Corporation) according to the manufacturer's instructions.

siRNA treatment

Two sets of siRNA against CDCP1 were synthesized and purchased from Life Technologies Corporation as described elsewhere (12). The control siRNA for CDCP1 was synthesized as follows: CDCP1 control siRNA-1, 5′-GCUACCGGAGCGAAACAACAUCUUA-3′ (sense), and 5′-UAAGAUGUUGUUUCGCUCCGGUAGC-3′ (antisense). siRNAs (40 pmol) were incorporated into cells using Lipofectamine 2000 or Oligofectamine (Life Technologies Corporation), according to the manufacturer's instructions. The cells were subjected to further experiments 72 hours after the siRNA treatment.

Plasmids, antibodies, and reagents

To generate the GFP-MT1-MMP construct, human MT1-MMP cDNA was subcloned into the pEGFP-N1 vector (Clontech Laboratories Inc.; ref. 29). Human MT1-MMP having a FLAG-tag at the N-terminus (MT1-F) was subcloned into the pSG5 vector (Sigma; ref. 32). The polyclonal antibodies against CDCP1 and tyrosine-phosphorylated CDCP1 (Tyr734) were prepared as described previously (8). The anti-MT1-MMP antibody (1D8) was prepared as described previously (33). Other antibodies used were α-tubulin (B-5-1-2; Sigma), cortactin (4F11; Millipore), caveolin-1 (610493; BD Biosciences), early endosome antigen 1 [EEA-1 (610457; BD Biosciences)], MT1-MMP (ab38971; Abcam), GFP (ab1218, Abcam; 04363-24, Nacalai Tesque), CDCP1 (ab1377; Abcam), Syntaxin 6 (C34B2; Cell Signaling Technology Inc.), and Tks5 (sc-9945; Santa Cruz Biotechnology).

Western blotting and immunoprecipitation

The Western blotting and immunoprecipitation were conducted as described previously (8). The cells were lysed with a buffer (20 mmol/L Tris-HCl, at pH 7.4, 150 mmol/L NaCl, 1 mmol/L EDTA, 20 mmol/L NaF, 1% Nonidet P-40, 5% glycerol, and 2% octyl-β-D-glucoside plus protease inhibitor) for dissolution of lipid rafts and subjected to Western blotting and immunoprecipitation. Protein concentration was determined using the Bicinchoninic Acid Protein Assay Kit (Thermo Fisher Scientific Inc.), and equal amounts of protein were separated by SDS-PAGE. A polyvinylidene difluoride membrane (Immobilon-P, Millipore) was used as the transfer membrane, and Blocking One (Nacalai Tesque) was used for blocking the membrane. For immunoprecipitation, 1 mg of protein was mixed with 5 μg of CDCP1 antibody and rotated with Protein G Sepharose beads (GE Healthcare) or 10 μL FLAG M2 agarose beads (Sigma).

Invadopodia assay

Fluorescent gelatin-coated coverslips were prepared as described previously (29, 34). MDA-MB-231 and RPMI 7951 cells were cultured for 3 to 7 hours on coverslips coated with fluorescent gelatin. In the case of the cells overexpressing MT1-MMP, they were cultured on the gelatin matrix for 2 hours. To quantitate the degradation activity of invadopodia, 20 randomly selected fields, usually containing 20 to 40 cells, were imaged with a × 60 objective for each determination. The degradation area was determined by using the ImageJ software version 1.41o and normalized for the number of cells. In each analysis, the mean value of the control cells was set at 100%, and the relative values of the cells treated with siRNAs were then calculated. The relative number of invadopodia per cell was determined by counting punctate F-actin structures that were positive for Tks5. The mean (SE) of at least 3 independent determinations was calculated.

Invasion assay

The invasion assay was conducted using modified Transwell chambers with a polycarbonate nucleopore membrane (BD Falcon), as described previously (8). The top side of the membrane was coated with 0.02% collagen (Cellmatrix Type I-A, Nitta Gelatin Inc.). The cells treated with each siRNA were seeded onto the top part of each chamber. After incubation for 30 hours, the cells on the membrane were fixed. The number of migrated or invaded cells was determined by counting the cells on the bottom side of the membranes from 2 wells (2 fields per membrane) at a magnification of × 100, and the extent of invasion was expressed as the average ratio (number of cells transfected with siRNA per field/average number of cells transfected with control siRNA per field). The results were expressed as the mean of 3 independent experiments.

Immunofluorescence

Immunofluorescence was conducted as previously described (34). Briefly, the cells were fixed in 4%

Published OnlineFirst February 25, 2013; DOI: 10.1158/1541-7786.MCR-12-0544

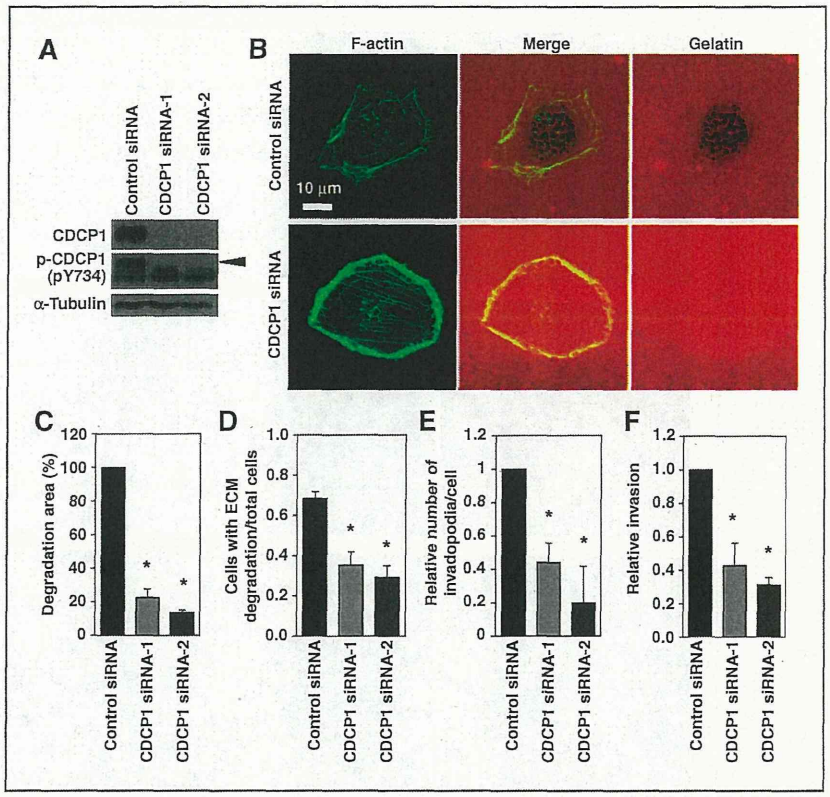

Figure 1. CDCP1 is required for invadopodia formation and ECM degradation by human breast cancer cells. A, the MDA-MB-231 cells were treated with control or CDCP1 siRNAs and subjected to Western blotting with the indicated antibodies. The black arrowhead shows CDCP1. B, the cells treated with the indicated siRNAs were cultured on fluorescent gelatin-coated coverslips for 7 hours and stained for F-actin. C, the areas showing degradation of the fluorescent gelatin matrix were quantified as described in the Materials and Methods. D, the proportion of the cells showing degradation of the gelatin matrix. E, the relative number of invadopodia per cell. F, the result of the invasion assay of the MDA-MB-231 cells treated with CDCP1 siRNAs. Columns, mean; bars, SD. *, $P < 0.05$.

paraformaldehyde for 15 minutes and permeabilized with 0.1% Triton X-100 for 5 minutes. The cells were blocked in 1% bovine serum albumin and 1% goat serum for 30 minutes, incubated with primary antibodies for 1 hour, and then incubated with Alexa Fluor-conjugated secondary antibodies and phalloidin (Life Technologies Corporation) for 30 minutes. The samples were observed with an IX81-ZDC-DSU confocal microscope (Olympus) equipped with a cooled CCD camera (ORCA-ER, Hamamatsu Photonics), and the imaging system was driven by the MetaMorph software (Universal Imaging). All the images were acquired using × 60 (PLAPON60XO, NA 1.42) or × 100 oil objectives (UPLSAPO100XO, NA 1.4). The images were analyzed and processed with various software packages, including MetaMorph, ImageJ version 1.41o (NIH, Bethesda, MD; http://rsbweb.nih.gov/ij/), and Adobe Photoshop CS4. The relative distribution of CDCP1 at the cell periphery versus intracellular vesicles was determined by calculating the ratio between the fluorescence intensities of peripheral and perinuclear vesicular CDCP1 from confocal images. For colocalization analysis, Mander overlap coefficient was calculated using ImageJ with Just Another Colocalization Plugin. All calculations were conducted on 8 to 20 cells.

Labeling cells with CTxB

The cells cultured on gelatin-coated coverslips were washed with ice-cold PBS and incubated with 10 μg/mL Alexa Fluor-conjugated cholera toxin B subunit (CTxB; Life Technologies Corporation) in PBS for 20 minutes on ice. For the internalization experiments, the cells were labeled with CTxB in the growth medium for 20 minutes on ice and then incubated for the indicated times at 37°C. The cells were stained with anti-CDCP1 antibody as described previously.

Cell fractionation

Cell fractionation was conducted as described previously (29). The cytosolic fraction was extracted with the

Published OnlineFirst February 25, 2013; DOI: 10.1158/1541-7786.MCR-12-0544

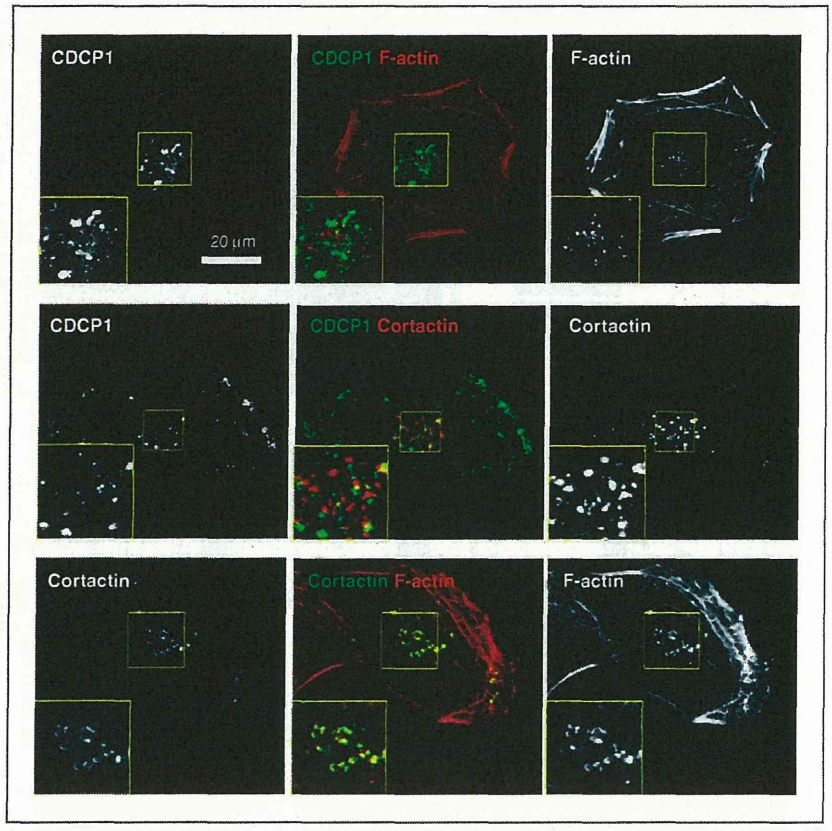

Figure 2. Localization of CDCP1 at invadopodia. The MDA-MB-231 cells were cultured on gelatin-coated coverslips and stained for CDCP1, cortactin, and F-actin. Top, F-actin (*red*) and CDCP1 (*green*); middle, cortactin (red) and CDCP1 (green); bottom, F-actin (red) and cortactin (green). The inserts are the magnified images of the boxed regions.

ProteoExtract Subcellular Proteome Extraction Kit (Millipore). Triton X-100 soluble materials were then extracted with a buffer (25 mmol/L Tris-HCl at pH 7.5, 150 mmol/L NaCl, 5 mmol/L EDTA, and protease inhibitors) containing 1% Triton X-100. Insoluble materials were further extracted with TNE buffer containing 1% SDS. Equal amounts of protein from each fraction were analyzed by immunoblotting.

Results

CDCP1 regulates invadopodia-mediated ECM degradation

The expression of CDCP1 in various cancers, including breast cancer, has been reported previously (7). We examined several human breast cancer cell lines and detected significant CDCP1 expression in MDA-MB-453, BT549, and MDA-MB-231 cells, using Western blotting (Supplementary Fig. S1). The immunoblotting with a phospho-specific antibody against Y734 of CDCP1 revealed tyrosine phosphorylation of CDCP1 in the highly invasive cell line BT549 and MDA-MB-231 (Fig. 1A and Supplementary Fig. S1), suggesting that CDCP1-mediated signaling might play a role in breast cancer cell invasion. Because invadopodia formation in MDA-MB-231 cells has been reported previously (35), we used this cell line to investigate the potential role of CDCP1 in invadopodia formation and function.

MDA-MB-231 cells were treated with 2 independent siRNAs against CDCP1 and subjected to Western blotting, which showed that CDCP1 expression was successfully suppressed by both siRNAs (Fig. 1A). The siRNA-treated cells were cultured on coverslips coated with fluorescent gelatin and tested for invadopodia formation and gelatin degradation. Gelatin degradation, which was primarily localized to the area around the invadopodia in MDA-MB-231 cells, was significantly decreased by treatment with CDCP1 siRNA, as shown by immunofluorescence and quantitative analysis of the degradation area (Fig. 1B and C). In addition, the proportion of cells with apparent degradation of the gelatin matrix was clearly decreased by CDCP1 knockdown (Fig. 1D). We also observed that CDCP1 knockdown significantly suppressed degradation of gelatin matrix by RPMI 7951 human melanoma cells (Supplementary Fig. S2A and S2B). It is known that assembly of actin-core structures and subsequent focal concentration of MMPs are both required for ECM degradation by invadopodia. The number of invadopodia that were punctate F-actin structures positive for an invadopodia marker Tks5 per cell was significantly decreased in cells transfected with CDCP1 siRNA (Fig. 1E). These observations indicate that CDCP1

Published OnlineFirst February 25, 2013; DOI: 10.1158/1541-7786.MCR-12-0544

is required for both assembly of invadopodia structures and ECM degradation activity. In addition, reduced expression of CDCP1 significantly suppressed invasion of MDA-MB-231 cells through Matrigel (Fig. 1F), which is consistent with our results obtained with gastric and pancreatic cancer cell lines (8, 12). Taken together, these results indicate that CDCP1 is an essential regulator of invadopodia-mediated ECM degradation during cancer cell invasion.

CDCP1 localizes to lipid raft-containing vesicular structures associated with invadopodia

To determine the cellular localization of CDCP1 in MDA-MB-231 cells, we conducted immunocytostaining with a specific antibody against CDCP1. Distinct signals for CDCP1 were observed as punctate and vesicular structures within the cells, and the signals were also detected at the cell periphery (Fig. 2). Quantitative analysis of fluorescence intensities showed that the ratio between perinuclear vesicular and peripheral CDCP1 was 0.42 ± 0.12 (SD, $N = 23$). These CDCP1 signals did not colocalize with invadopodia, which were observed as punctate structures at the cell-matrix adherent site showing positive staining for the invadopodia markers F-actin and cortactin. Nevertheless, strong vesicular CDCP1 signals were consistently observed in close proximity to invadopodia.

To identify the vesicular structures containing CDCP1, we conducted immunofluorescence analysis with several organelle markers. Syntaxin 6 is a *trans*-Golgi network protein and regulates membrane trafficking (36). Partial colocalization of CDCP1-containing vesicles with syntaxin

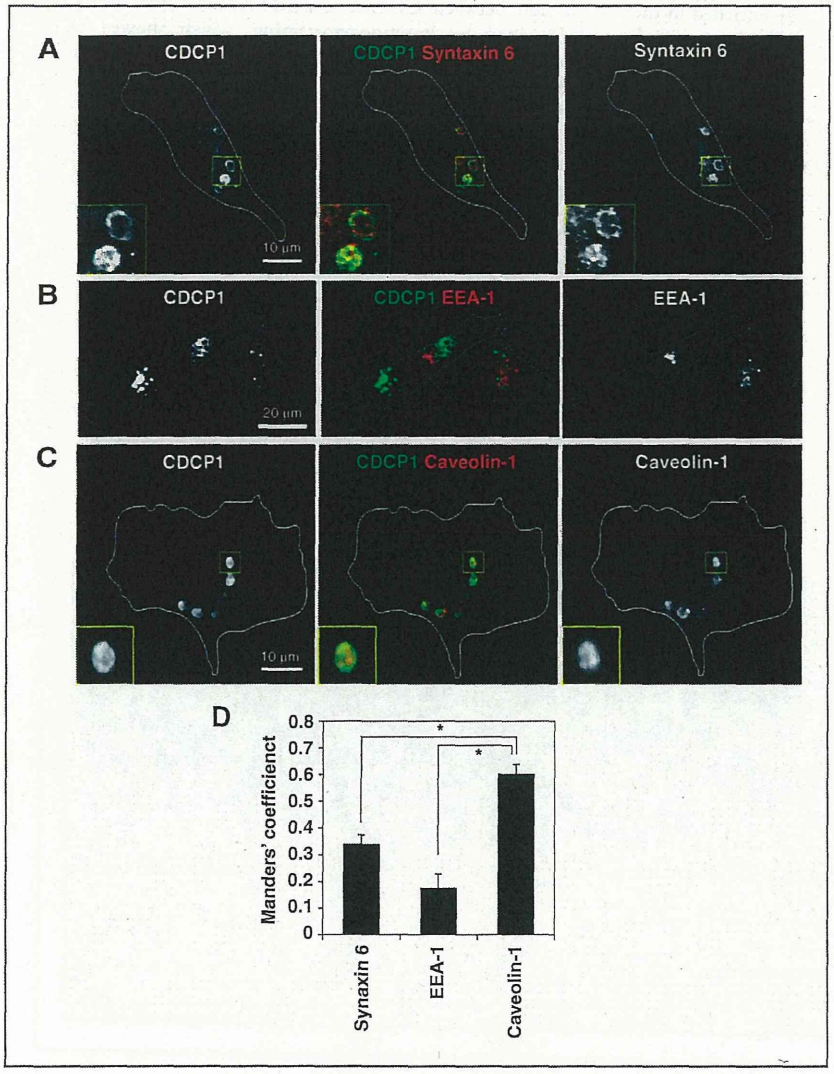

Figure 3. CDCP1 localizes to intracellular vesicles containing caveolin-1. The MDA-MB-231 cells were cultured on gelatin-coated coverslips and costained for CDCP1 with syntaxin 6 (A), EEA-1 (B), and caveolin-1 (C). Inserts are magnified images of the boxed regions. D, Mander coefficient was calculated on the basis of the degree of colocalization between CDCP1 and each vesicular marker from confocal immunofluorescence micrographs. Columns, mean; bars, SE. *, $P < 0.00001$.

Published OnlineFirst February 25, 2013; DOI: 10.1158/1541-7786.MCR-12-0544

6 (Fig. 3A) indicated that CDCP1 proteins are delivered through and/or function in the *trans*-Golgi network. CDCP1 did not colocalize with EEA-1, an early endosome marker (Fig. 3B), whereas it markedly colocalized with caveolin-1 in vesicular structures (Fig. 3C). Quantitative analysis of confocal images confirmed these observations and showed significant colocalization of CDCP1 with caveolin-1 (Fig. 3D).

Caveolin-1, an essential component of a subtype of lipid rafts called caveolae, regulates the organization and dynamics of lipid rafts and plays a role in membrane trafficking by regulating caveola/raft-dependent endocytosis (37). To determine whether CDCP1 is present in lipid rafts, MDA-MB-231 cells cultured on gelatin-coated dishes were separated into cytosolic, Triton X-100–soluble, and Triton X-100–insoluble fractions, and analyzed by Western blotting (Fig. 4A). Lipid rafts are known to be enriched in the Triton X-100–insoluble fraction (38, 39). As expected, CDCP1 was hardly detected in the cytosolic fraction but was concentrated in the Triton X-100–soluble membrane fraction. It is important to note that a significant amount of CDCP1 was also detected in the Triton X-100–insoluble fraction (Fig. 4A), indicating that CDCP1 exists in lipid rafts. Cells were then labeled with fluorescent CTxB, a lipid raft marker (40), and the course of CTxB internalization and localization of CDCP1 was simultaneously followed by immunofluorescence (Fig. 4B). Before the internalization, CTxB signals partly colocalized with CDCP1 at the ventral surface of the cell. The internalization of CTxB caused a shift of CTxB fluorescence to intracellular endosomes, where it colocalized with CDCP1 signals, starting 10 minutes after internalization and lasting until at least 60 minutes (Fig. 4B). Quantitative analysis of colocalization of CDCP1 and CTxB confirmed these observations (Fig. 4C). These results indicate that CDCP1 mainly exists in vesicular compartments where internalized lipid raft membranes accumulate.

CDCP1 colocalizes and associates with MT1-MMP

We previously reported that caveolin-1 colocalizes with MT1-MMP at lipid raft-enriched vesicles and regulates ECM degradation by invadopodia (29). The possible interaction between CDCP1 and MT1-MMP was therefore examined by immunocytostaining, which showed that MT1-MMP colocalized with CDCP1 at the vesicular structures (Fig. 5A). Mander coefficient for the degree of CDCP1 signals colocalizing with MT1-MMP was 0.63 ± 0.039 (SE, $N = 17$), which was very similar to that for CDCP1 colocalizing with caveolin-1 (Fig. 3D). In addition, the coimmunoprecipitation analysis conducted using MDA-MB-231 cells treated with octyl glucoside, which solubilizes

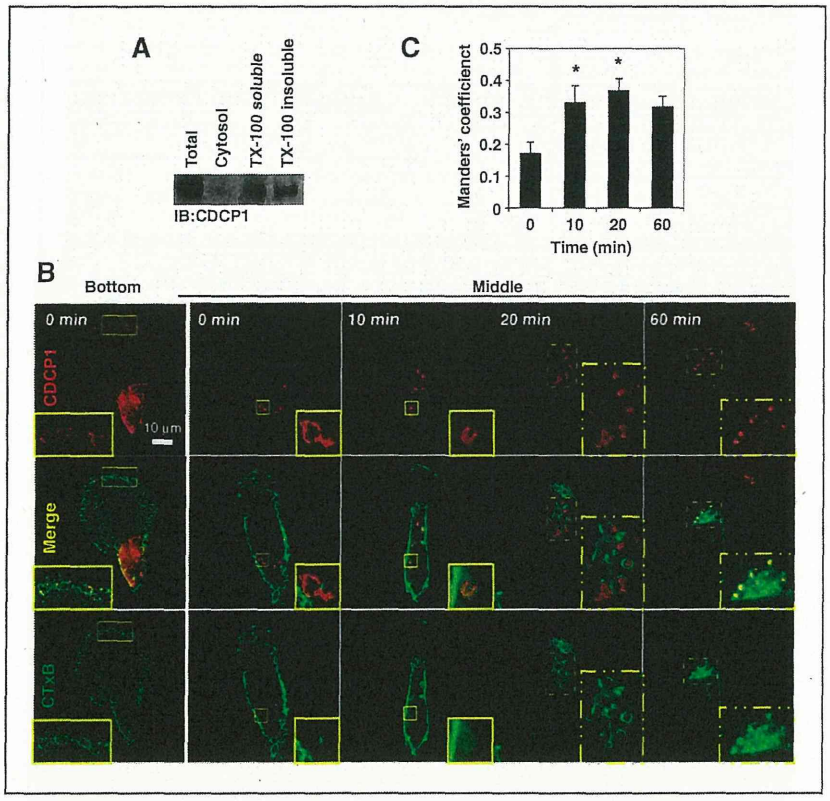

Figure 4. CDCP1 localizes to intracellular vesicles containing lipid rafts. A, the MDA-MB-231 cells were directly lysed or separated into cytosolic and Triton X-100–soluble and Triton X-100–insoluble fractions. The presence of CDCP1 in each fraction was determined by immunoblotting. B, the MDA-MB-231 cells cultured on gelatin-coated coverslips were labeled with fluorescent CTxB on ice and incubated at 37°C for the indicated time to allow internalization of CTxB. The cells were then stained with an anti-CDCP1 antibody. Before internalization (0 minute), CDCP1 was mainly detected in the intracellular vesicles (middle) and partly at the cell periphery, where it colocalized with CTxB (bottom). As internalization proceeded (10–60 minutes), CTxB signals were detected in the intracellular vesicles colocalized with CDCP1. The inserts are magnified images of the boxed regions. C, Mander coefficient was calculated to determine the degree of colocalization between CDCP1 and CTxB at different time points. Columns, mean; bars, SE. *, $P < 0.01$.